Localization of Noncovalently Bound Ethidium in Free and Methionyl-tRNA Synthetase Bound $tRNA^{fMet}$ by Singlet-Singlet Energy Transfer†

Blair Q. Ferguson‡ and David C. H. Yang*
Department of Chemistry, Georgetown University, Washington, D.C. 20057
Received February 19, 1986; Revised Manuscript Received April 23, 1986

ABSTRACT: Ethidium binds $tRNA^{fMet}$ with 17-fold enhancement in the emission intensity at 600 nm. Fluorescence titration of $tRNA^{fMet}$ with ethidium indicates a single high-affinity site in $tRNA^{fMet}$ with a dissociation constant of 5 μM. Ethidium is apparently rigidly bound to $tRNA^{fMet}$ and effectively shielded from solvent. $tRNA^{fMet}$(8–13), $tRNA^{fMet}$(3′-Flc), and $tRNA^{fMet}$(D-PF) with fluorophores at thiouridine, the 3′-terminus, and dihydrouridine, respectively, are prepared, and the singlet–singlet energy-transfer efficiencies between these fluorophores and noncovalently bound ethidium are determined. The transfer efficiency between bound ethidium and the fluorophore in $tRNA^{fMet}$(8–13) determined by donor quenching and sensitized emission is the same, strongly suggesting that there is only one bound ethidium per $tRNA^{fMet}$ molecule. The apparent distances between ethidium and various fluorophores including 3′-fluorescein, the 8–13 photo-cross-link, and D–proflavin are 41, 19, and 30 Å, respectively, assuming random orientation between the donor and the acceptor. The results suggest that noncovalently bound ethidium is intercalated in the amino acid acceptor stem. In the complex of $tRNA^{fMet}$ and methionyl-tRNA synthetase, the transfer efficiencies for the $tRNA^{fMet}$(8–13), $tRNA^{fMet}$(3′-Flc), and $tRNA^{fMet}$(D-PF) are reduced, enhanced, and little changed, respectively. These methionyl-tRNA synthetase induced changes suggest changes in the conformation of the 3′-terminal unpaired bases and the relative orientation or location between $tRNA^{fMet}$ and ethidium upon binding of methionyl-tRNA synthetase.

Interaction of tRNA and cognate synthetases has provided an excellent model system for the understanding of nucleic acid–protein interaction [for a review, see Schimmel & Soll (1979)]. Methionyl-tRNA synthetase and $tRNA^{fMet}$ appear to be one of the best systems, since the crystal structures of both methionyl-tRNA synthetase (Risler et al., 1981; Zelwer et al., 1982) and $tRNA^{fMet}$ (Woo et al., 1980) have been elucidated. The recognition of $tRNA^{fMet}$ and methionyl-tRNA synthetase likely involves mutual conformational adaptation [e.g., Krauss et al. (1976)] after the initial combination to eventually establish a stable tRNA–synthetase complex. The structure of the complex of methionyl-tRNA synthetase and $tRNA^{fMet}$ has been studied extensively by photo-cross-linking (Ackerman et al., 1985), ribonuclease susceptibility (Wrede et al., 1979), chemical modification and affinity labeling [e.g., Schulman et al. (1981) and Wetzel & Soll (1977)], neutron scattering (Dessen et al., 1982), and fluorescence spectroscopy (Blanquet et al., 1973). However, the nature of the involved conformational changes is not well understood. In order to define the involved conformational changes in $tRNA^{fMet}$ upon binding of methionyl-tRNA synthetase and to add definitive structural constraints to the tRNA–synthetase complex, we have carried out singlet–singlet energy-transfer experiments using fluorescence-labeled tRNA.

Singlet–singlet energy transfer has been used successfully as a spectroscopic ruler in a variety of biological systems [for a review, see Stryer (1978)]. Since the efficiency of energy transfer depends on the proximity as well as the relative orientation of the donor and the acceptor (Forster, 1966; Cantor & Schimmel, 1980), energy transfer provides a highly sensitive method for studying the conformational changes of macromolecules.

Noncovalently bound ethidium is used as the acceptor, since ethidium showed a single high-affinity site in tRNA (Bittman, 1969; Tao et al., 1970), dramatic fluorescence enhancement upon binding of tRNA, and good spectral overlap with several fluorescence derivatives of tRNA. Unfortunately, the precise location of the ethidium binding site in tRNA in solution has not been clearly established. X-ray crystallographic data of crystals of yeast $tRNA^{Phe}$ into which ethidium was allowed to diffuse showed that ethidium locates in the P10 cavity (Liebman et al., 1977) and partially stacks in a nonintercalative mode over S8. Some NMR data indicated that ethidium intercalates between the base pairs AU6 and AU7 of the acceptor stem in yeast $tRNA^{Phe}$ (Jones & Kearns, 1975; Jones et al., 1978), but others have favored the nonintercalative mode of binding (Liebman et al., 1977; Hurd & Reid, 1979). The intercalative mode appears to be consistent with the singlet–singlet energy transfer data for a 3′-dansylated $tRNA^{Phe}$ (Wells & Cantor, 1977). More recently, Thomas et al. (1984) have proposed that intercalated ethidium is at the strong binding site, while the nonintercalative binding corresponds to a weak binding site. In this paper, we report the results of energy transfer in three fluorescence derivatives of $tRNA^{fMet}$ to noncovalently bound ethidium in free tRNA and in the tRNA–synthetase complex.

Materials and Methods

Ethidium bromide, proflavin, fluorescein isothiocyanate, hydrazine, and acrylamide were from Sigma. Sodium cyanoborohydride was from Aldrich. All other chemicals were reagent-grade or the purest form available from standard sources.

Aminoacylation assay and fluorescence measurements including fluorescence titration, anisotropy, and dynamic quenching were carried out as previously described (Ferguson

† This work was supported by grants from NIH (GM-25848) and NSF (PCM 81-10818).
* Address correspondence to this author.
‡ Present address: Du Pont Experimental Station, Wilmington, DE 19898.

0006-2960/86/0425-5298$01.50/0

& Yang, 1986a). Preparation and characterization of fluorescent-labeled tRNA^{fMet}, including tRNA^{fMet}(3′-Flc),[1] tRNA^{fMet}(8–13), and tRNA^{fMet}(D-PF), have been described (Ferguson & Yang, 1986a). Titrations of MetRS and fluorescence-labeled tRNA were carried out and analyzed as previously described (Ferguson & Yang, 1986a). All steady-state fluorescence measurements were carried out in 10 mM Tris-HCl (pH 7.5), 10 mM $MgCl_2$, and 10 mM β-mercaptoethanol. The concentration of the enzyme stock solution is 18 μM.

Fluorescence Titration for Ethidium Binding. Binding of ethidium to tRNA^{fMet} was analyzed by using the enhancement of the ethidium emission or sensitized emission at varying concentration of tRNA^{fMet} (ΔF) and saturating concentration of tRNA^{fMet} (ΔF_{max}). After these are combined with the equation of conservation of mass and the Scatchard equation, eq 1 can be derived:

$$\frac{\Delta F}{\Delta F_{max}} = \frac{(nE_0 + X_0 + K) - [(nE_0 + X_0 + K)^2 - 4nE_0X_0]^{1/2}}{2X_0} \quad (1)$$

where E_0, X_0, n, and K are the total concentration of tRNA^{fMet}, the total concentration of ethidium, the binding stoichiometry, and the dissociation constant.

Binding of ethidium to fluorescent-labeled tRNA^{fMet} was also analyzed by monitoring the donor emission quenching at varying concentrations of ethidium ($\Delta F'$) and saturating concentration of ethidium ($\Delta F'_{max}$). After these are combined with the equation of conservation of mass and the Scatchard equation, eq 2 can be derived (Packmann et al., 1973; Engel, 1974):

$$\frac{\Delta F'}{\Delta F'_{max}} = \frac{(nE_0 + X_0 + K) - [(nE_0 + X_0 + K)^2 - 4nE_0X_0]^{1/2}}{2nE_0} \quad (2)$$

where E_0, X_0, n, and K are the total concentration of tRNA^{fMet}, the total concentration of ethidium, the binding stoichiometry, and the dissociation constant. The same equation is also applicable to the analysis of the binding data from monitoring the sensitized emission of ethidium.

Measurement of Energy-Transfer Efficiency. The noncovalently bound ethidium in tRNA^{fMet} is used as the emission acceptor for energy transfer with fluorescent-labeled tRNA^{fMet} in the absence and presence of MetRS. Since ethidium and MetRS are not covalently bound to tRNA^{fMet}, titrations with an increasing amount of ethidium or MetRS were carried out to determine the transfer efficiency of the complexes.

The apparent transfer efficiency (E_D) was measured as the extent of quenching of the donor emission by (Fairclough & Cantor, 1978)

$$E_D = 1 - F^D_{DA}(\lambda^{ex}_D,\lambda^{em}_D)/F^D_D(\lambda^{ex}_D,\lambda^{em}_D) \quad (3)$$

where $F^D_{DA}(\lambda^{ex}_D,\lambda^{em}_D)$ and $F^D_D(\lambda^{ex}_D,\lambda^{em}_D)$ are the emission intensity of donor in the presence and in the absence of the acceptor with the excitation wavelength (λ^{ex}_D) and the emission wavelength (λ^{em}_D) of the donor. The excitation and emission spectra of the donors are not shifted in the presence of ethidium in the present cases. Inner filter effect and dilution are corrected.

The apparent transfer efficiency was also determined from the sensitized emission by (Fairclough & Cantor, 1978)

$$E_A = \frac{A^A_{DA}(\lambda_D)}{A^D_{DA}(\lambda_D)}\left[\frac{F^A_{DA}(\lambda^{ex}_D,\lambda^{em}_A)}{F^D_A(\lambda^{ex}_D,\lambda^{em}_A)} - 1\right] \quad (4)$$

where $A^A_{DA}(\lambda_D)$ and $A^D_{DA}(\lambda_D)$ are the absorbances of the acceptor and the donor at the donor's absorption wavelength of the sample with both donor and acceptor and $F^A_{DA}(\lambda^{ex}_D,\lambda^{em}_A)$ and $F^D_A(\lambda^{ex}_D,\lambda^{em}_A)$ are the intensity of the sensitized emission and the acceptor emission at the emission wavelength of the acceptor and the excitation wavelength of the donor. The intensity of the sensitized emission was corrected for the contribution of donor emission with species containing donor only. The absorbance of the donor or acceptor was obtained from the respective extinction coefficient, the absorption spectrum (using Cary 14), the molar concentration of tRNA, and the labeling stoichiometry. The absorbance of noncovalently bound ethidium in tRNA^{fMet} was used to calculate the absorbance of the acceptor. For a given energy-transfer experiment, all measurements for different samples were carried out at the same time with identical instrumental settings to minimize necessary corrections.

The apparent transfer efficiency from eq 3 or 4 was corrected for the acceptor binding stoichiometry by

$$E_{cor} = E_{app}/f_A \quad (5)$$

where E_{app}, E_{cor}, and f_A are the apparent transfer efficiency (E_A or E_D), the corrected transfer efficiency, and the fraction of tRNA^{fMet} containing acceptor.

Calculation of Apparent Distances. The relation of the transfer efficiency of singlet–singlet energy transfer and the proximity between donor and acceptor has been shown (Forster, 1966; Cantor & Schimmel, 1980) as

$$R = (1/E - 1)^{1/6}R_0 \quad (6)$$

where $R_0 = [(8.79 \times 10^{-5})K^2n^{-4}\phi_D J_{DA}]^{1/6}$ and R and E are the apparent distance and the transfer efficiency. The overlap integral J was computed by numerical integration. The refractive index n was taken as 1.4 (Fairclough & Cantor, 1978). Quantum yield of the donor, ϕ_D, was determined from the relative quantum yield and corrected emission spectra (Cantley & Hammes, 1976) and was corrected for the polarization effect (Shinitzky, 1972).

The orientation factor K^2 was treated according to Haas et al. (1978) and Dale et al. (1979). The anisotropy of the fluorophores in fluorescent-labeled tRNA^{fMet} has been previously determined (Ferguson & Yang, 1986a).

Results

tRNA^{fMet}(Etd). The Etd fluorescence quantum yield increases dramatically and the excitation and emission wavelength maxima are significantly shifted upon addition of tRNA^{fMet} (Table I). The Scatchard plot in Figure 1 shows that Etd binds at a single site in tRNA^{fMet} with an equilibrium dissociation constant of 5 μM. This is in accord with the values reported for the binding of Etd to unfractionated yeast tRNA (Sakai & Cohen, 1976).

The relative emission intensity of tRNA^{fMet}-bound and free Etd at 600 nm (λ_{ex} = 500 nm) was determined to be 17. The emission lifetime of Etd is increased from 1.8 ns for free Etd to 24 ns for tRNA^{fMet}-bound Etd (data not shown). tRNA^{fMet}-bound Etd is effectively shielded from solvent molecules as indicated by the effect of D_2O on the Etd emission

[1] Abbreviations: Flc, fluorescein; PF, proflavin; Etd, ethidium; MetRS, methionyl-tRNA synthetase; tRNA^{fMet}(8–13), tRNA^{fMet} with reduced, photo-cross-linked S8–C13; tRNA^{fMet}(3′-Flc), tRNA^{fMet} with fluorescein thiosemicarbazide at 3′-terminus; tRNA^{fMet}(D-PF), tRNA^{fMet} with D20 replaced with proflavin; Tris-HCl, tris(hydroxymethyl)-aminomethane hydrochloride.

Table I: Fluorescence Properties of Free Etd and Etd Bound in $tRNA^{fMet}$

property	sample: Etd	sample: noncovalent $tRNA^{fMet}$-bound Etd
excitation wavelength maxima, λ_{max}^{ex} (nm)	285, 480	305, 515
emission wavelength maxima, λ_{max}^{em} (nm)[a]	615 (632)	595
relative emission intensity, F/F_0, at 600 nm (λ_{ex} = 500 nm)	1.0	17
emission lifetime, τ (ns)	1.8	24[b]
emission anisotropy, r[c]	0.017	0.137[d]
limiting anisotropy, r_0[e]	0.130	(0.287)
rotational relaxation time, τ(ns)[f]	0.27	22
relative quantum yield	1.0	14
relative quantum yield in H_2O and D_2O, D_2O/H_2O	3.7	1.4

[a] The values are taken from spectra that have not been corrected for the wavelength dependence of fluorometer detection system sensitivity. The value in parentheses is the corrected value (Wintermeyer & Zachau, 1979). [b] The contribution of free Etd to the emission decay was resolved with a two-exponential fit of the emission decay data. [c] Determined in standard buffer, at 590 nm (λ_{ex} = 510 nm), and at 20 °C. [d] Corrected for the contribution of free dye. [e] Determined from the intercept of the Perrin plot. The value of $tRNA^{fMet}$-bound Etd was assumed to be equal to that for the D-Etd fluorophore in $tRNA^{fMet}$-(D-Etd). [f] Calculated with eq 3 in Ferguson and Yang (1986a).

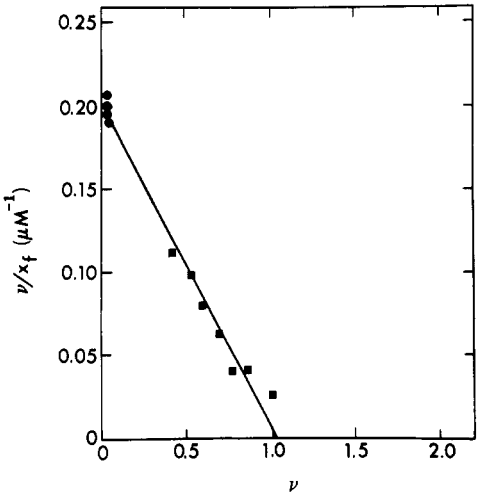

FIGURE 1: Scatchard plot of titration of $tRNA^{fMet}$ with ethidium. Titrations were carried out by adding $tRNA^{fMet}$ to ethidium (●) as well as with addition of ethidium to tRNA (■). The solid line is obtained for binding of Etd to a single site on $tRNA^{fMet}$, with an equilibrium dissociation constant, K, equal to 5.0 μM.

intensity (Olmsted & Kearns, 1977). The emission intensity of $tRNA^{fMet}$-bound Etd is increased by a factor of 1.4 in D_2O, relative to H_2O, whereas the emission intensity of free Etd is increased by a factor of 3.7.

The steady-state anisotropy for $tRNA^{fMet}$-bound Etd, at 20 °C, was determined to be 0.137 at 590 nm (λ_{ex} = 510 nm). The rotational correlation time for $tRNA^{fMet}$-bound Etd is calculated to be 22 ns, suggesting that Etd is rigidly bound to $tRNA^{fMet}$, with little or no local rotational freedom independent of the tRNA molecule. Fluorescence properties of free and $tRNA^{fMet}$-bound Etd are summarized in Table I.

$tRNA^{fMet}$ with noncovalently bound Etd at the single, highly fluorescent site is designated $tRNA^{fMet}$(Etd), which was typically prepared by mixing a saturating amount of Etd with $tRNA^{fMet}$. $tRNA^{fMet}$(Etd) can be fully aminoacylated with methionine by MetRS, to the same extent as $tRNA^{fMet}$ in the absence of Etd. The rate of aminoacylation of $tRNA^{fMet}$(Etd), however, was reduced 75% relative to that for $tRNA^{fMet}$ in

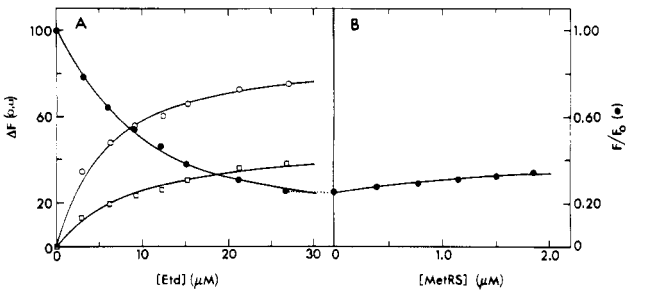

FIGURE 2: (A) Fluorescence titration of 1.5 μM $tRNA^{fMet}$(8–13) with Etd. The emission intensity was monitored for donor quenching (●) at 460 nm (λ_{ex} = 390 nm), for sensitized emission (□) at 590 nm (λ_{ex} = 400 nm), and for total ethidium emission (○) at 590 nm (λ_{ex} = 520 nm). The intensity at 460 nm is plotted as F/F_0 (right scale), where F_0 is the initial 8–13 emission intensity in the absence of Etd. The intensity at 590 nm (λ_{ex} = 400 nm) and 590 nm (λ_{ex} = 520 nm) is plotted as ΔF (left scale). The binding parameters of the fitting functions [wavelength monitored, K (μM), $(F/F_0)_{max}$ or ΔF_{max}, and n, respectively] are as follows: 460 nm (λ_{ex} = 390 nm), 7.6, 0.04, 1.0; 590 nm (λ_{ex} = 400 nm), 4.6, 88, 1.0; 590 nm (λ_{ex} = 520 nm), 7.8, 48, 1.0. (B) The fluorescence titration with MetRS for the sample at the end of the titration in (A) containing 1.4 μM $tRNA^{fMet}$(8–13) and 27 μM Etd. The emission intensity was monitored for donor quenching (F/F_0) at 460 nm (λ_{ex} = 390 nm). The binding parameters of the fitting curve are K = 0.11 μM, $\Delta(F/F_0)_{max}$ = 0.10, and n = 1.0.

the absence of Etd, in agreement with a previous report (Kearns, 1976). $tRNA^{fMet}$(Etd) quenches MetRS tryptophan fluorescence to the same extent as $tRNA^{fMet}$ and binds to MetRS with close to the same affinity as $tRNA^{fMet}$, as determined from MetRS tryptophan quenching data (data not shown). These data suggest that the interaction of $tRNA^{fMet}$(Etd) with MetRS is very similar to that of unmodified $tRNA^{fMet}$.

The emission intensity of $tRNA^{fMet}$-bound Etd is quenched up to 7% upon binding of $tRNA^{fMet}$(Etd) to MetRS (data not shown). This small change suggests that Etd remains bound in $tRNA^{fMet}$(Etd) and reflects induced conformation changes in $tRNA^{fMet}$ surrounding Etd when $tRNA^{fMet}$ is complexed with MetRS. MetRS by itself did not change the emission intensity of Etd.

$tRNA^{fMet}$(8–13,Etd). The fluorescence titration of $tRNA^{fMet}$(8–13) with Etd is shown in Figure 2A. The quenching of the donor (8–13) emission was monitored at 460 nm (λ_{ex} = 390 nm). At the end of the titration, F_{DA}^D/F_D^D (cf. eq 3), which is equivalent to F/F_0, is 0.25. The transfer efficiency determined by donor quenching, E_D, is thus 0.75. At this point in titration, the extent of Etd binding of $tRNA^{fMet}$ is 0.78. The transfer efficiency corrected for the acceptor labeling stoichiometry (0.78), E_D^{cor} (cf. eq 5), is calculated to be 0.96.

The transfer efficiency for 8–13 and bound Etd was also determined from the sensitized emission at 590 nm (λ_{ex} = 400 nm, Figure 2A). At the end of the titration, the sensitized emission is 7.0-fold greater than that of unmodified $tRNA^{fMet}$ with Etd under the same conditions. On the basis of eq 4, the transfer efficiency determined by sensitized emission, E_A, is calculated to be 0.73. The energy-transfer efficiency determined by donor quenching, E_D, and that from sensitized emission, E_A, are, therefore, in close agreement. This result shows that the quenching of the 8–13 emission results from energy transfer and that there is indeed only one high-affinity site for Etd in $tRNA^{fMet}$. Furthermore, the binding parameters for the ethidium binding to $tRNA^{fMet}$(8–13) as determined by donor quenching or sensitized emission are the same and are nearly identical with those determined from Etd emission from the binding of Etd to unmodified $tRNA^{fMet}$. Thus, the

Table II: Energy-Transfer Parameters for Free and MetRS-Bound tRNA^{fMet}(8–13,Etd), tRNA^{fMet}(3′-Flc,Etd), and tRNA^{fMet}(D-PF,Etd)

parameter	free tRNA^{fMet}-(8–13,Etd)	MetRS-bound tRNA^{fMet}-(8–13,Etd)	free tRNA^{fMet}-(3′-Flc,Etd)	MetRS-bound tRNA^{fMet}-(3′-Flc,Etd)	free tRNA^{fMet}-(D-PF,Etd)	MetRS-bound tRNA^{fMet}-(D-PF,Etd)
donor	8–13	8–13	3′-Flc	3′-Flc	D-PF	D-PF
acceptor	tRNA^{fMet}-bound Etd	tRNA^{fMet}-bound Etd	tRNA^{fMet}-bound Etd	tRNA^{fMet}-bound Etd	tRNA^{fMet}-bound Etd	tRNA^{fMet}-bound Etd
J (M^{-1} cm^{-1} nm^4)	1.3×10^{14}	1.3×10^{14}	3.0×10^{14}	3.0×10^{14}	2.9×10^{14}	2.9×10^{14}
ϕ_D	0.60	0.60	0.84	0.50	0.13	0.14
$R_0(^2/_3)$ (Å)[b]	33	33	40	37	29	29
E_D	0.75	0.65	0.35	0.51	0.36	0.31
E_A	0.73	nd	(0.20)	nd	(0.20)	nd
f_A (mol of acceptor/mol of tRNA^{fMet})	0.78	0.75	0.80	0.78	0.82	0.80
E_D^{cor}	0.96	0.88	0.44	0.65	0.45	0.39
$R(^2/_3)$ (Å)[b]	19.3	23.7	41.7	33.3	30.2	31.3
$R(^2/_3)/R$[b]	0.89–1.10	0.89–1.13	0.91–1.08	0.91–1.11	0.91–1.11	0.89–1.13
R (Å)	19.2 ± 2	23.8 ± 2.8	42.5 ± 3.5	32.5 ± 4.5	30.5 ± 3	31 ± 4

[a] The parameters are defined under Materials and Methods: J, spectral overlap; ϕ_D, quantum yield of donor; $R_0(^2/_3)$, characteristic distance; E_D, transfer efficiency by donor quenching; E_A, transfer efficiency by sensitized emissions; f_A, fractional occupancy of Etd; E_D^{cor}, corrected transfer efficiency; $R(^2/_3)$, apparent distance separating the donor and the acceptor; $R(^2/_3)/R$, range of ratios of distances with the probability parameter (Q) of 0.5 and the apparent distance based on the anisotropy of the fluorophores according to Haas et al. (1978); R, range of distances with the probability parameter (Q) of 0.5. [b] $(^2/_3)$ denotes that the orientation factor (K^2) is assumed to be $^2/_3$ for the calculation of apparent distance.

same strong binding site appears to be monitored in all cases. Due to the nature of the involved variables used to determine E_D and E_A, E_D can be determined with greater precision than E_A. For this reason, only the change in E_D was monitored in the titration of tRNA^{fMet}(8–13,Etd) with MetRS.

Upon addition of MetRS to tRNA^{fMet}(8–13,Etd), the 8–13 quenching by Etd is reduced from 66% to 52% (Figure 2B). Since the emission intensity of the fluorophore in tRNA^{fMet}(8–13) is not changed upon binding of MetRS in the absence of Etd (Ferguson & Yang, 1986a), the MetRS-induced change in F/F_0 shown in Figure 2B is equivalent to the change in F_{DA}^D/F_D^D for the 8–13 donor and the tRNA^{fMet}-bound Etd acceptor. The binding of tRNA^{fMet}(8–13,Etd) to MetRS reduces the corrected energy-transfer efficiency from 0.96 to 0.83. The energy-transfer parameters for free and MetRS-bound tRNA^{fMet}(8–13,Etd) are summarized in Table II.

tRNA^{fMet}(3′-Flc,Etd). The fluorescence titration of tRNA^{fMet}(3′-Flc) with Etd is shown in Figure 3A. The extent of donor quenching, F/F_0, is equivalent to F_{DA}^D/F_D^D. At the end of the titration, F_{DA}^D/F_D^D is 0.65, which corresponds to E_D of 0.35. The transfer efficiency corrected for the acceptor labeling stoichiometry (0.80), E_D^{cor}, is calculated to be 0.44.

The energy-transfer efficiency determined from the sensitized acceptor emission E_A was found to be significantly less than E_D (Table II). However, E_A could not be measured reliably in this system, due to the relatively high emission from the saturating amount of free Etd. It cannot be excluded that 3′-Flc emission is quenched by other processes, in addition to Forster energy transfer to bound Etd. For this reason, the value of E_D determined for this system may be considered a maximum limiting value for energy transfer between the 3′-Flc and Etd.

The extent of MetRS-induced quenching of 3′-Flc emission (Ferguson & Yang, 1986a) is increased in the presence of Etd in comparison to that in the absence of Etd (data not shown). After correction for the MetRS-induced quenching in 3′-Flc emission intensity due to the change in local environment of fluorescein [by dividing each value of F/F_0 in the presence of ethidium by the corresponding value in the absence of ethidium for the titration of tRNA^{fMet}(3′-Flc)], the change in energy transfer, F_{DA}^D/F_D^D, for the 3′-Flc donor and tRNA^{fMet}-bound Etd acceptor can be obtained. As shown in Figure 3B, upon binding of tRNA^{fMet}(3′-Flc,Etd) to MetRS,

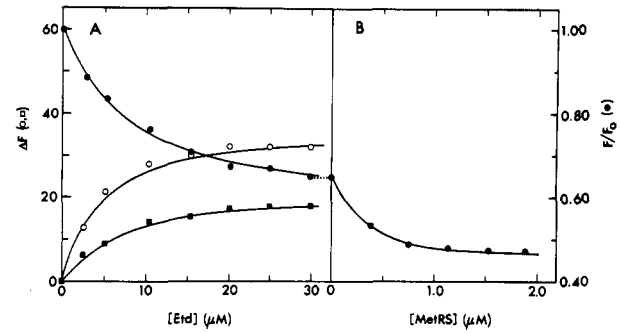

FIGURE 3: (A) Fluorescence titration of 0.37 μM tRNA^{fMet}(3′-Flc) with Etd. The emission intensity, F, was monitored for donor quenching (●) at 520 nm (λ_{ex} = 480 nm), for sensitized emission (□) at 600 nm (λ_{ex} = 480 nm), and for total ethidium emission (○) at 600 nm (λ_{ex} = 520 nm). The intensity at 520 nm is plotted as F/F_0 (right scale). The intensity at 600 nm (λ_{ex} = 480 nm) and 600 nm (λ_{ex} = 520 nm) is plotted as ΔF (left scale). The binding parameters for the functions fitting the data [wavelength monitored, K (μM) $(F/F_0)_{max}$ or F_{max}, and n, respectively] are as follows: 520 nm (λ_{ex} = 480 nm), 7.5, 0.56, 1.0; 600 nm (λ_{ex} = 480 nm), 4.1, 38, 1.0; 600 nm (λ_{ex} = 520 nm), 7.2, 23, 1.0. (B) Fluorescence titration with MetRS of the sample at the end of the titration in (A), containing 0.35 μM tRNA^{fMet}(3′-Flc) and 30 μM Etd. The emission intensity was monitored for donor quenching (F/F_0) at 520 nm (λ_{ex} = 480 nm). The data were corrected for the MetRS-induced quenching of 3′-Flc emission in the absence of Etd due to the change in the local environment of 3′-fluorescein. The binding parameters of the function fitting the data are K = 0.11 μM, $\Delta(F/F_0)_{max}$ = –0.20, and n = 1.0.

energy-transfer efficiency to the Etd acceptor is increased from 35% to 51%. After correction for the fractional occupancy of ethidium in tRNA, the transfer efficiency corresponds to 0.64. The energy-transfer parameters for free and MetRS-bound tRNA^{fMet}(3′-Flc,Etd) are summarized in Table II.

tRNA^{fMet}(D-PF,Etd). The fluorescence titration of tRNA^{fMet}(D-PF) with Etd is shown in Figure 4A. At the end of the titration, the extent of D-PF quenching, F/F_0 (F_{DA}^D/F_D^D) is 0.64, which corresponds to a transfer efficiency of 0.36. At this point in the titration, the extent of Etd binding on tRNA^{fMet} is 0.80.

The transfer efficiency for the D-PF donor and tRNA^{fMet}-bound acceptor determined from the sensitized acceptor emission, E_A, is found to be 0.20. The value is significantly less than that determined by donor quenching (E_D), suggesting that the donor may be quenched by other processes

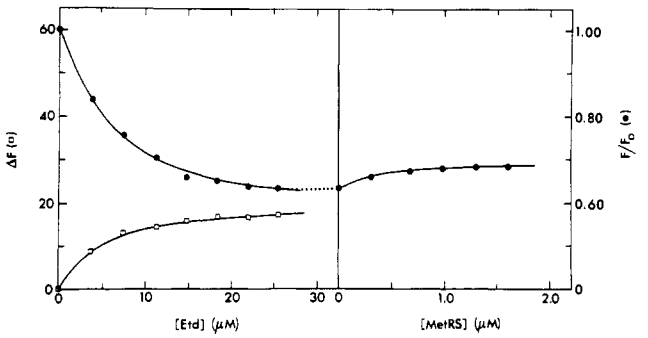

FIGURE 4: (A) Fluorescence titration of 0.36 μM tRNA^{fMet}(D-PF) with Etd. The emission intensity, F, was monitored for donor quenching (●) at 500 nm (λ_{ex} = 455 nm) and for sensitized emission (□) at 600 nm (λ_{ex} = 455 nm). The donor emission at 500 nm (λ_{ex} = 455 nm) is plotted as F/F_0 (right scale), where F_0 is the initial D-PF emission intensity in the absence of Etd. The sensitized emission at 600 nm (λ_{ex} = 455 nm) is plotted as ΔF (left scale). The binding parameters for the functions fitting the data [wavelength monitored, K (μM), $(F/F_0)_{max}$ or F_{max}, and n, respectively] are as follows: 500 nm (λ_{ex} = 455 nm), 5.8, 0.55, 1.0; 600 nm (λ_{ex} = 455 nm), 4.7, 21, 1.0. (B) Fluorescence titration with MetRS of the sample at the end of the titration in (A), containing 0.35 μM tRNA^{fMet}(D-PF) and 25 μM Etd. The emission intensity was monitored at 500 nm (λ_{ex} = 455 nm). The data have been corrected for the MetRS-induced increase in D-PF emission due to the MetRS-induced change in the local environment of PF. The binding parameters of the function fitting the data are K = 0.14 μM, $(F/F_0)_{max}$ = 0.05, and n = 1.0.

in addition to Forster energy transfer.

The titration of tRNA^{fMet}(D-PF,Etd) with MetRS, as monitored by the donor quenching, is shown in Figure 4B. The MetRS-induced increase in D-PF emission due to the change in the local environment of PF has been corrected (Ferguson & Yang, 1986a). As shown in Figure 4B, upon binding of tRNA^{fMet}(D-PF,Etd) to MetRS, the extent of quenching of D-PF emission due to energy transfer to the Etd acceptor is decreased from 36% to 31%. The energy-transfer parameters determined for free and MetRS-bound tRNA^{fMet}(D-PF,Etd) are summarized in Table II.

Discussion

tRNA^{fMet} shows a strong binding site for ethidium, as demonstrated by the enhancement of the ethidium emission. The affinity of ethidium toward tRNA^{fMet} is comparable to that of ethidium intercalation in DNA or double-stranded RNA (Waring, 1965). The present results of singlet–singlet energy transfer between bound ethidium and tRNA^{fMet}(8–13) excluded the possibility of significant binding of ethidium without fluorescence enhancement under the conditions used, since donor quenching and sensitized emission gave nearly identical transfer efficiencies. The universality of ethidium binding in tRNA has been suggested on the basis of its existence and identical locations in tRNA^{Phe} and unfractionated tRNA (Wells & Cantor, 1977). The presence of such a single strong binding site provides an excellent fluorescent probe.

Particularly efficient energy transfer was observed by use of the bound Etd acceptor and the donor fluorophore in tRNA^{fMet}(8–13) by monitoring either donor quenching or sensitized emission. Such highly efficient energy transfer has not been previously demonstrated by sensitized emission in biological macromolecules. It is well-known that the transfer efficiency depends on the proximity, spectral overlap, orientation, sizes, shape, rotational freedom, and spatial distribution of the emission and absorption dipoles of the donor and the acceptor groups (Forster, 1966; Cantor & Schimmel, 1980). In practice, an apparent distance, assuming random orientation, and the most likely range of distance are calculated on the basis of the transfer efficiency, the characteristic distance (R_0), and the anisotropy of the fluorophores (Haas et al., 1978; Dale & Eisinger, 1979). The apparent distance between bound ethidium and 8–13 in tRNA^{fMet}, if the fluorophores are assumed to be randomly oriented, is calculated to be 19.2 Å. The range of probable distance is 17.2–21.2 Å (cf. Table II), by use of a probability parameter (Q) (Haas et al., 1978) of 0.5.

Upon binding of methionyl-tRNA synthetase, the efficiency of energy transfer between ethidium and 8–13 in tRNA^{fMet} was significantly reduced, suggesting conformational changes at the local environment of 8–13 or the ethidium binding site. The apparent distance [$R(^2/_3)$] is calculated to be 23.7 Å (cf. Table II). This large change is rather surprising since only small fluorescence changes in tRNA^{fMet}(8–13) or tRNA^{fMet}(Etd) were observed upon binding of methionyl-tRNA synthetase (Ferguson & Yang, 1986). The enzyme-induced conformational changes surrounding 8–13 have, however, been indicated by the reduced rate of photo-cross-linking between S8 and C13 in tRNA^{Phe} upon binding of cognate synthetase (Holler et al., 1981). Nonetheless, the fact that S8 and C13 can be photo-cross-linked in the presence of cognate synthetase suggests that their relative position remains close to each other. It appears more likely that bound ethidium has changed its orientation or location in tRNA^{fMet} upon binding of MetRS.

With tRNA^{fMet}(3′-Flc), an apparent distance of 42 Å separating 3′-fluorescein and bound ethidium is obtained (cf. Table II). This value is close to the apparent distance (33–40 Å) previously reported for tRNA^{Phe} with dansylhydrazide covalently attached at the 3′-terminus (Wells & Cantor, 1977).

Upon binding of MetRS to tRNA^{fMet}(3′-Flc), the transfer efficiency between 3′-Flc and Etd is appreciably increased. This increase in transfer efficiency corresponds to a reduction of the apparent distance between the fluorophores by as much as 9 Å, assuming random orientation between the donor and the acceptor. MetRS-induced conformational changes at the 3′-terminus have previously been observed by the large reduction in the emission intensity, solvent accessibility, and rotational freedom of fluorescein at the 3′-terminus (Ferguson & Yang, 1986). In the crystal structure of tRNA^{Phe}, the last five unpaired nucleotides at the 3′-terminus are extended away from tRNA in a continuing helix (Kim et al., 1974; Robertus et al., 1974). In contrast, the corresponding nucleotides are folded back toward tRNA in the crystal structure of tRNA^{fMet} (Woo et al., 1980). Anisotropy measurements showed that the 3′-terminus is highly flexible in free tRNA and is rigid upon binding of MetRS. The present energy transfer data suggest that the 3′-terminal nucleotides may be partially folded back toward the acceptor stem in the tRNA–synthetase complex.

The transfer efficiency in tRNA^{fMet}(D-PF) with bound ethidium corresponds to an apparent distance of 30 Å separating the donor and the acceptor, assuming random orientations (cf. Table II). Upon binding of MetRS, the transfer efficiency to ethidium was slightly reduced, corresponding to an increase of 1 Å between the fluorophores. This is expected on the basis of the fact that the fluorescence properties of the corresponding tRNA labeled with a single fluorophore showed little changes upon binding of MetRS. However, since the large changes in the transfer efficiency of tRNA^{fMet}(8–13) and tRNA^{fMet}(3′-Flc) to ethidium were observed, the small change in the case of tRNA^{fMet}(D-PF) may be a fortuitous balance in the change in the proximity and orientation such that no net change in transfer efficiency was observed.

Table III: Comparison of Apparent Distances from Ethidium Binding Site Based on Energy Transfer and Crystallographic Data

	distances (Å)			
	energy transfer[a]		crystallographic data[b]	
	-MetRS	+MetRS	AU6–AU7	P10 pocket
3′-terminus	41	33	37	50
8–13	19	24	15	6
D20	30	31	25	15

[a] The orientation factor K^2 is assumed to be $^2/_3$. [b] Measurements using yeast tRNA^{Phe} and an on-line computer display program developed by Dr. B. K. Lee (NIH).

Conflicting results on the precise location of bound ethidium in tRNA have been obtained as described in the introduction. The present results are compared to the predicted distances based on the yeast tRNA^{Phe} crystal structure for intercalative and nonintercalative modes of binding (Table III). Keeping all the limitations of energy transfer in mind, the present results appear to favor the intercalative mode for the ethidium binding. The 3′-terminus is 50 Å from the nonintercalative ethidium site and about 37 Å from AU6 and AU7 base pairs (or base pairs GC6 and GC7 in tRNA^{fMet}), on the basis of an extended conformation for the 3′-terminal nonpaired nucleotides. The apparent distances of ethidium from 8–13 and D20 are much farther than those predicted for the nonintercalative site and are close to the predicted distances for the intercalation site. Taken together, the present results of energy-transfer experiments exclude the nonintercalative site as the ethidium binding site in tRNA^{fMet} in solution. The intercalative site appears to be between base pairs GC6 and GC7. However, intercalation between base pairs GC5 and GC6 or GC4 as the predominant site is also within the range of the distance measurements. The energy-transfer measurements cannot resolve these possibilities.

Upon binding of MetRS, the transfer efficiency to ethidium for tRNA^{fMet}(3′-Flc) was enhanced, and that of tRNA^{fMet}-(8–13) was reduced, while that of tRNA^{fMet}(D-PF) showed little change. These changes in transfer efficiency reflect conformational changes in tRNA^{fMet} or perhaps the interaction of ethidium with tRNA^{fMet}. Since tRNA^{fMet}(Etd) showed little quenching in ethidium upon binding of MetRS, it appears that ethidium remains bound in the same high-affinity site as in free tRNA^{fMet}.

As discussed earlier, the decrease of the apparent distance from the 3′-terminus to the ethidium site may be due to the folding of the 3′-unpaired nucleotides toward the amino acid acceptor stem in the tRNA–synthetase complex. A similar interpretation was proposed on the basis of the neutron scattering studies (Dessen et al., 1982). However, this folded-back conformation remains to be elucidated. A simultaneous increase in the apparent distance from the 8–13 cross-link to the ethidium site was observed upon binding of methionyl-tRNA synthetase. Movement of ethidium in tRNA^{fMet} toward the 3′-terminus could simultaneously decrease the distance to the 3′-end and increase the distance to 8–13 without changing its distance to D20. The crystal structure of the ethidium–dinucleotide complex showed that intercalation of ethidium between base pairs stretches the neighboring base pairs by the distance of an additional base pair (Tsai et al., 1975). Free tRNA apparently can accommodate the intercalation of ethidium by spanning the base pairs GC6 and GC7. In the tRNA–synthetase complex, however, the 3′-terminus must be in justaposition at the active site of the enzyme, while sU8 forms a covalent intermediate with the enzyme (Starzyk et al., 1982). Conformational changes near the ethidium site or a delocalized conformation change in the acceptor stem may be necessary in order to relieve the strain introduced from the intercalation of ethidium. As a result, the observed changes in the transfer efficiency may be in part due to the movement of ethidium in its orientation or sliding in between the base pairs. It appears that bound ethidium changes its orientation such that the energy transfer became favorable toward 3′-Flc and unfavorable toward 8–13. Assuming there is no change in the proximity between 3′-fluorescein and ethidium, the orientation factor, K^2, would have to increase about 4-fold (e.g., 0.16 to 0.64) to compensate for the observed increase in transfer efficiency. Unfortunately, energy-transfer analysis cannot distinguish changes due to orientation or proximity.

In summary, the present results evidently suggest that ethidium intercalates in the amino acid acceptor stem in tRNA^{fMet}. The results for the tRNA–synthetase complex suggest that the 3′-terminus becomes immobilized in a partially folded-back conformation and that ethidium is likely reoriented toward the 3′-end. The synthetase-induced conformational change in tRNA^{fMet} can be further defined with the methodology developed here. Further studies using tRNA^{fMet} with two covalently attached fluorescence groups may add additional conformational constraints to the structure of tRNA–synthetase complex (Ferguson & Yang, 1986b). Such results should be helpful in eventually building a model for the tRNA–synthetase complex from the known crystal structures of tRNA^{fMet} and MetRS.

ACKNOWLEDGMENTS

We gratefully acknowledge the discussion with Dr. B. K. Lee (NIH) and the use of the display program in the analysis of the crystallographic data of tRNA^{Phe}.

Registry No. Ethidium, 3546-21-2.

REFERENCES

Ackerman, E. J., Joachimiak, A., Klinghofer, V., & Sigler, P. (1985) *J. Mol. Biol. 181*, 93–102.

Bittman, R. (1969) *J. Mol. Biol. 46*, 251–268.

Blanquet, S., Iwatsubo, M., & Waller, J. P. (1973) *Eur. J. Biochem. 36*, 213–226.

Blanquet, S., Dessen, P., & Fayat, G. (1979) in *Transfer RNA: Structure, Properties and Recognition* (Abelson, J., Schimmel, P., & Soll, D., Eds.) pp 281–299, Cold Spring Harbor Laboratory, Cold Spring Harbor, NY.

Cantley, L. C., & Hammes, G. G. (1976) *Biochemistry 15*, 1–14.

Cantor, C. R., & Schimmel, P. R. (1980) in *Biophysical Chemistry*, Freeman, New York.

Dale, R. E., & Eisinger, J. (1979) *Biophys. J. 26*, 161–194.

Dessen, P., Fayat, G., Zaccai, G., & Blanquet, S. (1982) *J. Mol. Biol. 154*, 603–613.

Engel, G. (1974) *Anal. Biochem. 61*, 184–191.

Fairclough, R. H., & Cantor, C. R. (1978) *Methods Enzymol. 48*, 347–379.

Fairclough, R. H., & Cantor, C. R. (1979) *J. Mol. Biol. 132*, 575–586.

Ferguson, B. Q., & Yang, D. C. H. (1986a) *Biochemistry 25*, 529–539.

Ferguson, B. Q., & Yang, D. C. H. (1986b) *Biochemistry* (in press).

Forster, T. (1966) in *Modern Quantum Chemistry* (Sinanoglu, O., Ed.) Section III, pp 93–137, Academic, New York.

Haas, E., Katzir, E. K., & Steinberg, I. Z. (1978) *Biochemistry 17*, 5064–5070.

Holler, E., Baltzinger, M., & Favre, A. (1981) *Biochemistry 20*, 1139–1147.
Hurd, R. E., & Reid, B. R. (1979) *Biochemistry 18*, 4005–4011.
Jones, C. R., & Kearns, D. R. (1975) *Biochemistry 14*, 2660–2665.
Jones, C. R., Bolton, P. H., & Kearns, D. R. (1978) *Biochemistry 17*, 601–607.
Kearns, D. R. (1976) *Prog. Nucleic Acid Res. Mol. Biol. 18*, 91.
Kim, S. H., Suddath, F. L., Quigley, G., McPherson, A., Sussman, N., Wang, A. H. L., & Rich, A. (1974) *Science (Washington, D.C.) 185*, 435–440.
Krauss, G., Riesner, D., & Maas, G. (1976) *Eur. J. Biochem. 68*, 81–93.
Liebman, M., Rubin, J., & Sandaralingam, M. (1977) *Proc. Natl. Acad. Sci. U.S.A. 74*, 4821–4825.
Olmsted, J., & Kearns, D. R. (1977) *Biochemistry 16*, 3647–3654.
Pachmann, U., Cronvall, E., Rigler, R., Hirsch, R., Wintermeyer, W., & Zachau, H. G. (1973) *Eur. J. Biochem. 39*, 265–273.
Rich, A., & Schimmel, P. R. (1977) *Nucleic Acids Res. 4*, 1649–1665.
Risler, J. L., Zelwer, C., & Brunie, S. (1981) *Nature (London) 292*, 384–386.
Robertus, J. D., Ladner, J. E., Finch, J. T., Rhodes, D., Brown, R. S., Clark, B. F. C., & Klug, A. (1974) *Nature (London) 250*, 546–551.
Rosa, J. J., Rosa, M. D., & Sigler, P. B. (1979) *Biochemistry 18*, 637–647.
Sakai, T. T., & Cohen, S. S. (1976) *Prog. Nucleic Acid Res. Mol. Biol. 17*, 15.
Schimmel, P. R., & Soll, D. G. (1979) *Annu. Rev. Biochem. 48*, 601–648.
Schulman, L. H., & Pelka, H. (1977) *Biochemistry 16*, 4256–4265.
Schulman, L. H. Valenzuela, D., & Pelka, H. (1981) *Biochemistry 20*, 6018–6023.
Shinitzky, M. (1972) *J. Chem. Phys. 56*, 5979–5981.
Starzyk, R. M., Koontz, S. W., & Schimmel, P. R. (1982) *Nature (London) 298*, 136–140.
Stryer, L. (1978) *Annu. Rev. Biochem. 47*, 819–846.
Tao, T., Nelson, J. H., & Cantor, C. R. (1970) *Biochemistry 9*, 3514–3524.
Thomas, G., Fourrey, J. L., & Favre, A. (1978) *Biochemistry 17*, 4500–4514.
Thomas, J. C., Schurr, J. M., & Hare, D. R. (1984) *Biochemistry 23*, 5407–5413.
Tsai, C. C., Jain, S. C., & Sobell, H. M. (1975) *Proc. Natl. Acad. Sci. U.S.A. 72*, 628–632.
Waring, M. J. (1965) *J. Mol. Biol. 13*, 269–282.
Wells, B. D., & Cantor, C. R. (1977) *Nucleic Acids Res. 4*, 1668–1680.
Wetzle, R., & Soll, D. (1977) *Nucleic Acids Res. 4*, 1681–1694.
Wintermeyer, W., & Zachau, H. G. (1979) *Eur. J. Biochem. 98*, 465–475.
Woo, N. H., Roe, B. A., & Rich, A. (1980) *Nature (London) 286*, 346–351.
Wrede, P., Woo, N. H., & Rich, A. (1979) *Proc. Natl. Acad. Sci. U.S.A. 76*, 3289–3293.
Zelwer, C., Risler, J. L., & Brunie, S. (1982) *J. Mol. Biol. 155*, 63–81.

Intermediates in the Biosynthesis of Coenzyme M (2-Mercaptoethanesulfonic Acid)†

Robert H. White
Department of Biochemistry and Nutrition, Virginia Polytechnic Institute and State University, Blacksburg, Virginia 24061
Received January 17, 1986; Revised Manuscript Received April 16, 1986

ABSTRACT: The early steps in the formation of coenzyme M (2-mercaptoethanesulfonic acid) were examined in purified extracts of *Methanobacterium formicicum*. Extracts incubated with phosphoenolpyruvate (PEP), bisulfite, and cysteine were found to readily catalyze the enzymatic formation of the coenzyme; incubation with pyruvate instead of PEP produced no coenzyme. Extracts were incubated with PEP, bisulfite, and cysteine and analyzed for the presence of sulfonic acids by gas chromatography–mass spectrometry (GC–MS) of suitable derivatives. Three of the proposed intermediates in the conversion of these products into coenzyme M were identified, i.e., sulfolactic acid, sulfopyruvic acid, and sulfoacetaldehyde. Sulfopyruvic acid was also shown to be readily converted into sulfoacetaldehyde and coenzyme M by the extracts. These results are consistent with the initial step in coenzyme M biosynthesis being the condensation of PEP with sulfite to form sulfolactic acid. The sulfolactic acid is then oxidized to sulfopyruvic acid which is decarboxylated to form sulfoacetaldehyde. After reaction with cysteine to form a thiazolidine intermediate, the sulfoacetaldehyde is subsequently converted into enzyme M by a series of known reactions (R. H. White, unpublished results).

The structure of coenzyme M (2-mercaptoethanesulfonic acid), one of several recently described coenzymes involved in the biological production of methane (Escalante-Semerena et al., 1984), was determined in 1974 by Taylor and Wolfe. It is unique among coenzymes in that it occurs only in methanogenic bacteria (Balch & Wolfe, 1979). It is also the smallest organic coenzyme (M_r 142), it contains the highest percentage of sulfur (45%), and it is one of the few sulfonic acids found in nature. The methylation of coenzyme M to

† This work was funded by National Science Foundation Grant PCM-8217072.

0006-2960/86/0425-5304$01.50/0